macaque monkeys because famous thalidomide as a limbs teratogen acts sensitively on the embryo of rhesus monkey in the period of 24-30 days after gestation [13]. The limb malformations with thalidomide also occur among macaque species including Japanese monkeys during almost same periods [14].

Above the results show dioxin isomers including TCDD may have no effects on the limb malformation when TCDD acts singly in the same period of thalidomide as a teratogen.
The limb malformations may be occurring with other material(s) or their complex in the living environments surrounding the monkeys. Those abnormalities are serious for humans because the physiological resemblance based on the molecular similarity between humans and monkeys. Further studies are necessary to clarify the materials and limb malformation relationships.

Figure 1: Provisional semi-wild monkey with congenital finger less in Japan

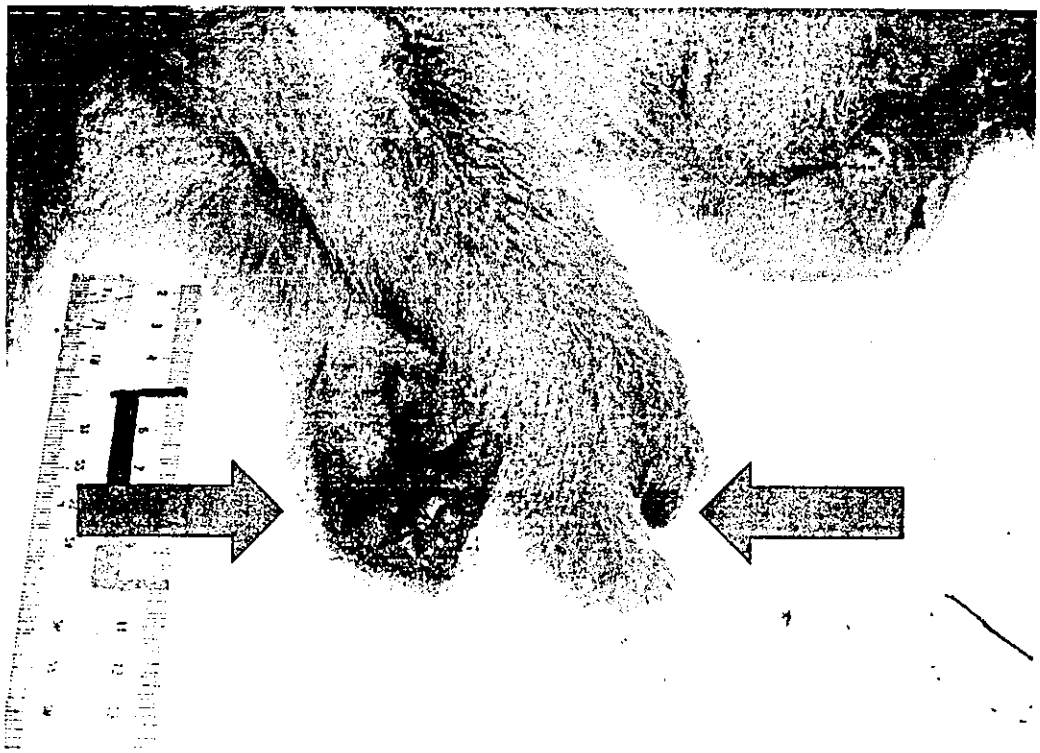

Figure 2: The comparison of TEQ in the blood of monkeys with between malformation limbs and normal limbs
☆A, abnormal; N, normal; f, female; m, male; number, birth year

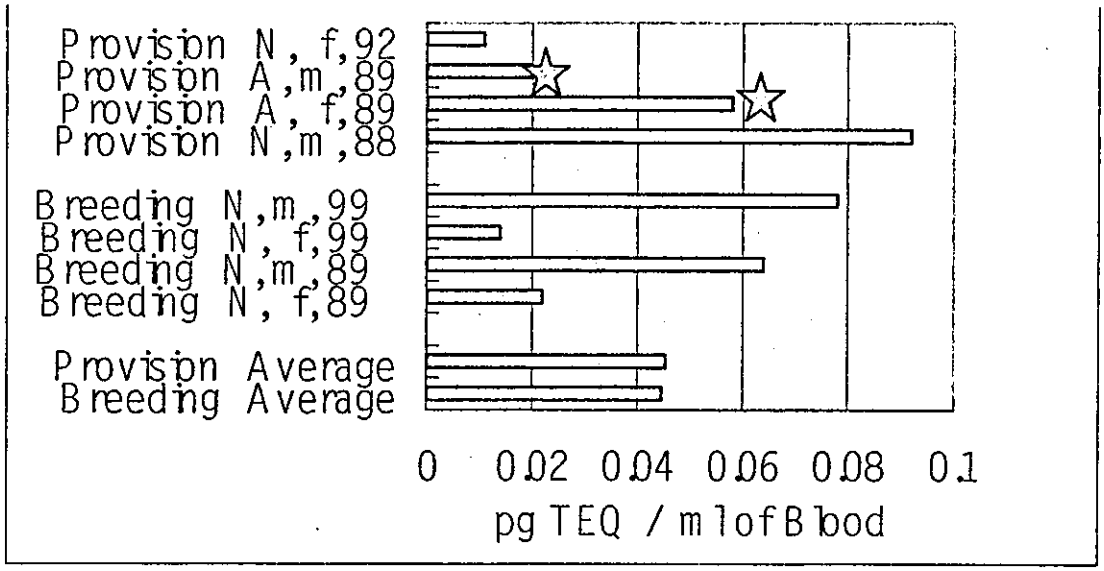

Acknowledgment
This study was supported by Health Labour Sciences Research Grants for Research on Food and Chemical Safety from the Ministry of Health Labour and Welfare of Japan, and MEXT Grant-in-Aid for Scientific Research from the Ministry of Education, Culture, Sports, Science and Technology of Japan.

References

1. Hagenmaier, H., Wiesmuller, T., Golor, G., Krowke, R., Heige, H. and Neubert, D. (1990) Arch Toxicol 64: 601-615
2. Kubota, K., Ihara, T., Sato, M., Takasuga, T., Yasuda, M., Fukusato, T., Hori, H., Nomizu, M., Kobayashi, T., Seyama, Y. and Nagata, R. (2000) Organohalogen Compounds 49: 255-258
3. Yasuda, M., Ihara, T., Takasuga, T., Kubota, S., Matsui, K., Yamashita, K. and Nagata, R. (2000) Organohalogen Compounds 49: 391-393
4. Kubota, K., Ihara, T., Oneda, S., Inoue, M., Sato, M., Takasuga, T., Yasuda, M., Fukusato, T., Hori, H., Nomizu, M., Kobayashi, T. and Nagata, R. (2001) Organohalogen Compounds 53: 88-91
5. Asaoka, K., Iida, H., Suzuki, J., Watanabe, K., Inoue, M., Fukusato, T., Murata, N., Nomizu, M., Nagata, R., and Kubota, S. (2003) Organohalogen Compounds, 64: 423-426
6. Yasuda, I., Yasuda, M., Sumida, H., Tsusaki, H., Inouye, M., Tsuga, K., and Akagawa, Y. (2003) Organohalogen Compounds, 64: 431-434
7. Itani, J. and Mizuhara, H. (1957) Bull. Exp. Anim., 4: 105-107 (in Japanese)
8. Yoshihiro, S., Goto, S., Minezawa, M., Muramatsu, M., Saito, Y., Sugita, H., and Nigi, H.(1979) Ecotox. Environ. Safe., 3: 458-470
9. Minezawa, M., Nozawa, K., Gotoh, S., Yoshihiro, S., Hamada, Y., Inagaki, H. and Nigi, H. (1990) Primates, 31: 571-577
10. Ihara, T., Oneda, S., Yamamoto, T., Boudrel, L., Lau, D., Miller, D., and Nagata, R. (1999) Cong Anom. 39, 383
11. Miettinen, H.M., Alaluussua, S., Tuomisto, J., and Viluksela, M. (2002) Toxicol. Appl. Pharmacol. 184: 57
12. Kiukkonen, A., Villuksela, M., Sahlberg, C., Alaluusua, S., Tuomisto, J.T., Tuomisto, J. and Lukinmaa, P.-L. (2002) Toxicol. Sci., 69: 482.
13. Wilson, J.G., and Gavan, J.A. (1967) Anat. Rec. 158: 99-110
14. Tamimura, T. (1972) Acta Endocrinol. 166 (Suppl.): 293-308

ELSEVIER

Mechanisms of Development 121 (2004) 1443–1453

www.elsevier.com/locate/modo

Mouse Nkd1, a Wnt antagonist, exhibits oscillatory gene expression in the PSM under the control of Notch signaling

Aki Ishikawa[a], Satoshi Kitajima[b], Yu Takahashi[b], Hiroki Kokubo[a], Jun Kanno[b], Tohru Inoue[b], Yumiko Saga[a,*]

[a]*Division of Mammalian Development, National Institute of Genetics, Yata 1111, Mishima 411-8540, Japan*
[b]*Cellular and Molecular Toxicology Division, National Institute of Health Sciences, 1-18-1 Kamiyoga, Setagayaku, Tokyo 158-8501, Japan*

Received 19 May 2004; received in revised form 29 July 2004; accepted 9 August 2004
Available online 16 September 2004

Abstract

During vertebrate embryogenesis, the formation of reiterated structures along the body axis is dependent upon the generation of the somite by segmentation of the presomitic mesoderm (PSM). Notch signaling plays a crucial role in both the generation and regulation of the molecular clock that provides the spatial information for PSM cells to form somites. In a screen for novel genes involved in somitogenesis, we identified a gene encoding a Wnt antagonist, Nkd1, which is transcribed in an oscillatory manner, and may represent a new member of the molecular clock constituents. The transcription of *nkd1* is extremely downregulated in the PSM of *vestigial tail* (*vt/vt*), a hypomorphic mutant of Wnt3a, whereas *nkd1* oscillations have a similar phase to *lunatic fringe* (*L-fng*) transcription and they are arrested in Hes7 (a negative regulator of Notch signaling) deficient embryos. These results suggest that the transcription of *nkd1* requires Wnt3a, and that its oscillation patterns depend upon the function of Hes7. Wnt signaling has been postulated to be upstream of Notch signaling but we demonstrate in this study that a Wnt-signal-related gene may also be regulated by Notch signaling. Collectively, our data suggest that the reciprocal interaction of Notch and Wnt signals, and of their respective negative feedback loops, function to organize the segmentation clock required for somitogenesis.

Keywords: Subtraction; Somitogenesis; Wnt signaling; Mesp2; Segmentation clock

1. Introduction

Somites are transient structures that are only observed during embryogenesis, and their reiterated nature in vertebrates is an important foundation for the generation of metameric structures such as vertebrae, ribs, spinal nerves and skeletal muscle. The somites are formed sequentially in an anterior to posterior direction, concomitant with the posterior extension of the tailbud. Once the paraxial mesoderm is generated from the tailbud, the cells are known to then be under the control of the segmentation clock (or molecular clock) and acquire periodic properties (Pourquié, 2001). Among the several genes that have been implicated in somitogenesis, those involved in the Notch signaling pathway are now known to play major roles. The experimental and genetic evidence that is now accumulating also indicates that Notch signaling is a component of the molecular clock that governs temporal control, and that it is also required for the establishment of the rostro-caudal polarity of somites within the presomitic mesoderm (PSM) prior to segment border formation (Takahashi et al., 2000). The molecular mechanisms underlying these events have recently begun to be more fully understood. There could, however, be additional genes and/or signaling pathways involved in somitogenesis. In fact, Wnt signaling is implicated in both the generation and maturation of tailbud cells (Takada et al., 1994), whereas FGF signaling has been shown to be important for the maintenance of immature PSM cells prior to segmentation (Dubrulle et al., 2001; Sawada, 2001).

Previously, we cloned the gene *Mesp2*, which encodes a bHLH-type transcription factor (Saga et al., 1997) and is

* Corresponding author. Tel: +81-559-81-6829; fax: +81-559-81-6828.
E-mail address: ysaga@lab.nig.ac.jp (Y. Saga).

0925-4773/$ - see front matter © 2004 Elsevier Ireland Ltd. All rights reserved.
doi:10.1016/j.mod.2004.08.003

transiently expressed in the rostral PSM (in either S-1 or S-2: we refer a forming somite as S0) before segment border formation occurs. Additionally, *Mesp2*-null mice show defective somitogenesis due to a lack of a rostral somitic compartment. Recent genetic analyses have also now revealed that *Mesp2* functions in a Notch-signaling feedback network (Takahashi et al., 2003). Mesp2 stimulates *Notch1* expression and suppresses *Dll1* expression, whereas both Notch 1 and Dll1 appear to be required for either the activation or maintenance of *Mesp2* expression. However, no direct targets of Mesp2 have yet been identified.

In order to identify putative downstream target genes of Mesp2 and to further elucidate the molecular mechanisms underlying the formation and maturation of PSM cells, which are required for somite segmentation, we generated two subtractive cDNA libraries and screened them by in situ hybridization (ISH). We subsequently obtained more than 30 clones that are expressed in either the somite, the PSM and/or the tailbud. Among these genes, we identified several known components of the Wnt signaling pathway, and we focused in particular on the mouse *nkd1* gene which is expressed in an oscillatory manner in the PSM. *nkd* is a homolog of the *Drosophila* segment polarity gene *naked cuticle* (*nkd*), which encodes an antagonist of Wg activity (Zeng et al., 2000). It has been shown that mouse Nkd1 can bind Dishevelled and antagonize canonical Wnt signaling (Yan et al., 2001a; Wharton et al., 2001). Furthermore, it has also recently been reported that *Axin2*, which encodes an inhibitor of Wnt signaling, exhibits a cyclic expression pattern during somitogenesis and may play a key role upstream of the segmentation clock generated by Notch signaling (Aulehla et al., 2003). Our comparative analyses of such cyclic genes suggest that *nkd1* is a component of these pathways that exhibits an oscillatory expression pattern, which may act as a link between the Notch and Wnt signaling cascades and contribute to the establishment of the segmentation clock.

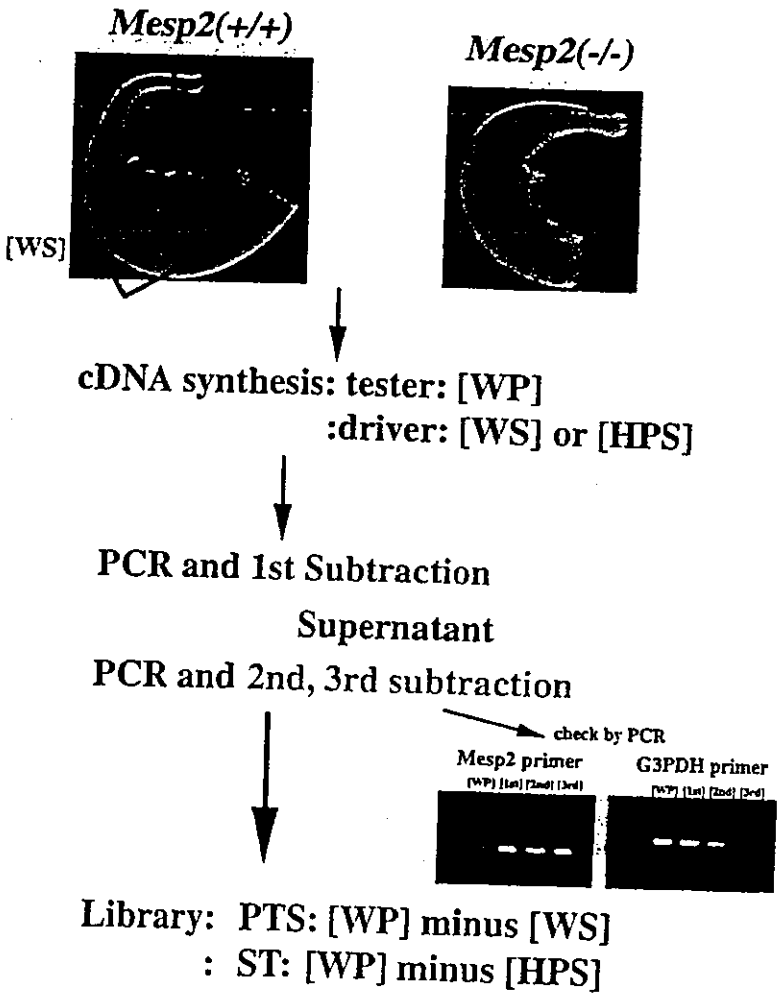

Fig. 1. Schematic representation of subtractive cDNA library protocols. Subtraction was carried out with cDNAs derived from the dissected portions of either wild-type (WP and WS) or Mesp2-null (HPS) 11.5 dpc embryos. Two different types of oligonucleotide linker-primers were utilized to prepare either tester or driver cDNAs. After three rounds of subtraction, the efficiency of the method was validated for the *Mesp2* (specific RNA to the PSM) and *G3PDH* (ubiquitous RNA) genes by PCR. After the cloning steps, we designated the generated subtractive libraries as PTS ([WP] minus [WS]) and ST ([WP] minus [HPS]).

Table 1
Characterization of somitic genes obtained using the subtractive strategy

Clone no.	Character	EP in WT	EP in Mesp2$^{-/-}$
ST347	Hes7	PSM (oscillates)	No change
ST371	laminin alpha 1	PSM (strong at S-1)	Expands anteriorly
ST556	Glcci1*	AER, somite, NT (dorsal)	No change
ST623	Laminin 5	PSM-1, somite anterior	Disappears
ST676	LEF1	PSM (strong at S-1)	Expands anteriorly (S-1 region)
ST686			
ST762			
PTS286			
PTS360			
ST313	Neuropilin-2	Rostral compartment of somites	Disappears
ST736	Axin2	PSM (oscillates) (S-1 region)	Expands anteriorly (S-1 region)
PTS124	SemaF-Cap3	PSM, somite	Downregulated
PTS338			
PTS149	DOC4/Nrg1	PSM, somite, head	No change
PTS179	Slit3	Tailbud, somite, DM	No change
PTS250	Hoxc13	Tailbud	No change
PTS426			
PTS607			
PTS363	Tropomyosin	Tailbud	No change
PTS378#	No gene prediction	PSM(S-1)	Upregulated
PTS474	ETV5	Tailbud, PSM(S0)	Downregulated (S0 region)
PTS485	MOCH**	somite posterior	No change
PTS542	Nkd2	PSM, somite (dorsal)	No change
PTS635	Calsyntenin-2	PSM(S-1), somite	No change
PTS646	Ets2	PSM (strong at S-1)	Downregulated

EP, expression pattern; WT, wild-type, PSM, presomitic mesoderm; AER, apical ectodermal ridge; NT, neural tube; DM, dermomyotome; *, glucocorticoid induced transcript1; **, mitochondrial oxodicarboxylate carrier homolog; #, GenBank accession number (AB178168).

2. Results

2.1. Screening strategy

Our study has two fundamental aims; to isolate and identify novel genes that are expressed specifically in the PSM and to characterize novel genes that function downstream of Mesp2. To accomplish these goals, we constructed two subtractive cDNA libraries, designated PTS and ST (Fig. 1). The enrichment of specific genes was validated by PCR, using either *G3PDH*- (a ubiquitously expressed gene) or *Mesp2*- (a PSM specific gene) specific primers. *G3PDH* cDNA was found to have been successfully depleted, whereas *Mesp2* cDNA was still evident after repeated subtractions (Fig. 1), suggesting that the subtractive hybridizations had worked effectively. After partial sequencing of randomly selected clones (406 for the PTS and 636 for the ST libraries), an initial search of the GenBank database in NCBI was done using blastn and known genes were removed. As a further screening strategy, we utilized the whole mount ISH technique, using the tail regions of 11.5 dpc embryos. The total number of clones that we subsequently screened by ISH were 251 and 280, for PTS and ST libraries, respectively.

After completion of the ISH screening, we identified more than 30 clones that showed expression in the somite and/or PSM regions. Further sequencing and homology searches using the Celera database identified some of these as regions of known genes (Table 1).

2.2. Characterization of genes obtained by subtractive hybridization

Blastn searches of the GenBank and Celera genome databases identified genes, such as *lymphoid enhancer factor-1* (*LEF1*), that were represented by a number of redundant clones. The clones ST676, PTS566, and PTS629 encode portions of *LEF1* cDNA and ST686, ST762, PTS286, and PTS360 were also identified as intronic sequences of the *LEF1* gene (Table 1 and Fig. 2). During this screening we often obtained intronic DNAs, probably due to the unspliced heterogeneous RNAs since we prepared RNA from whole cells containing nuclei. The intronic DNA fragments sometimes gave rise to different expression patterns, compared with those obtained using exon probes, and these were initially classified differently, as in the case of *LEF1*(Fig. 2) a known nuclear effecter of the Wnt/β-catenin signaling pathway (Porfiri et al., 1997; Hsu et al., 1998). The expression of intronic *LEF1* was observed as an intense band in either S-1 or S-2 of the PSM, in a pattern similar to *Mesp2*, and a lower intensity signal was also observed in the middle PSM. Interestingly the expression was expanded anteriorly in *Mesp2*-null embryos, which is also observed for several genes such as *L-fng* or *Dll1* (Nomura-Kitabayashi et al., 2002). The frequent appearance of this gene, showing these expression patterns, indicated that our strategy could successfully isolate genes that are specifically expressed in the PSM. This was also confirmed for the ST library, from which we isolated two clones, ST313 and ST623, which were identified as *neuropilin-2* and *laminin5*, respectively, and these expression profiles were observed to be confined to the rostral part of somites and are downregulated in Mesp2-null embryos (Table 1 and Fig. 2). Another ST clone, ST371 was identified to be an intronic sequence for *laminin alpha1*, which expression was expanded anteriorly in Mesp2-null embryos (Table 1 and Fig. 2).

Homology searches of the Celera database also determined that clone ST736 contained sequences encoding Axin2 (also named conductin) which functions as a negative regulator of Wnt signaling by inducing β-catenin degradation (Behrens et al., 1998). The expression pattern of

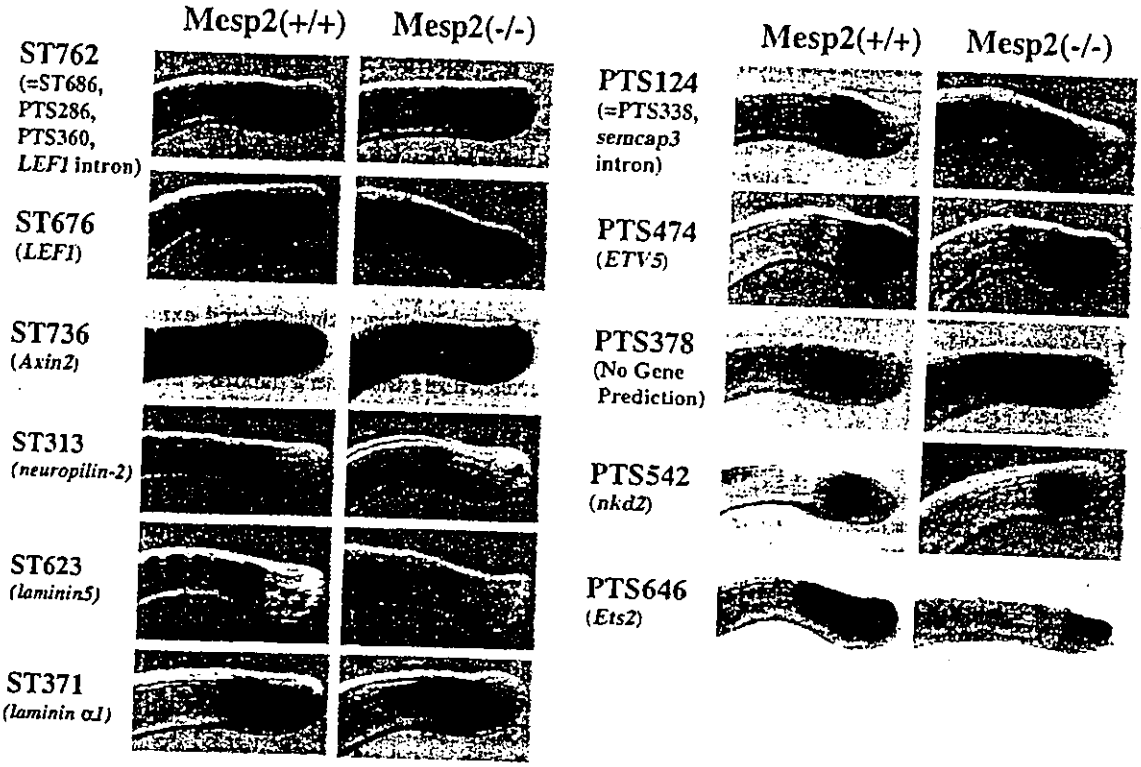

Fig. 2. Expression patterns of cDNA clones selected by ISH screening. ISH were performed with the tail region of wild-type embryos at 11.5 dpc (left side), in comparison to Mesp2-null mutants (right side).

mouse *Axin2* exhibits oscillation in the PSM (Aulehla et al., 2003), with different phase properties from those of *L-fng*, which is an oscillating gene in the Notch signaling pathway. Interestingly, although *Axin2* expression still oscillates when Notch signaling is impaired, a stable stripe of *Axin2* transcripts, in the anterior-most PSM of wild-type embryos, was not observed in Dll1-null mutants (Aulehla et al., 2003). We isolated this clone from our ST library, which may indicate that *Axin2* expression is controlled either directly or indirectly by Mesp2. As shown in Fig. 2, we also observed that the anterior stripe of the *Axin2* transcripts became diffuse and did not form a clear band in Mesp2-null embryos. Celera database searches indicated that the clones PTS124 and PTS338 were intronic sequences of '*M-SEM F cytoplasmic domain-associated protein 3*' (*semcap3*), the expression of which becomes diffuse in the Mesp2-null embryo (Fig. 2). A *Xenopus* homolog of the semcap/GIPC family, kermit, interacts directly with the cytoplasmic portion of the Wnt receptor, frizzled, via its PDZ domain and modulates its signaling activity (Rasmussen et al., 2001; Tan et al., 2001). However, semcap3 has low homology with other family members, and no function has so far been postulated for this protein. PTS474 was identified as '*Ets variant gene 5 (ETV5)*', encoding a transcription factor that contains an Ets DNA binding domain. *ETV5* is expressed in both the tailbud and middle PSM, but not in the anterior-most PSM, and this expression subsequently reappears at the segmental border (Fig. 2). In the Mesp2-null embryo, however, the anterior expression of *ETV5* becomes indistinct. Recently, it has been reported that mouse *ETV5* is expressed in the epithelium of the developing lung and plays a role in epithelial–mesenchymal interactions during lung organogenesis (Liu et al., 2003), but its function in the PSM is still unknown. PTS642 was identified to encode Ets2, another Ets-transcription factor and the expression is downregulated in Mesp2-null embryo (Fig. 2). The expression pattern during morphogenesis has been described (Ristevski et al., 2002). Targeted mutation of Ets2 is reported to result in embryonic lethal before 8.5 dpc due to the defective trophoblast function. However, rescued mice by aggregation with tetraploid embryos are viable and no defect in somitogenesis is reported (Yamamoto et al., 1998). Using either Celera or GenBank database searches, there was no homology detected between PTS378 and known genes. In addition, this clone is unique as it is up-regulated in the absence of Mesp2 (Fig. 2). which was a rare finding during our subtraction analyses. We speculate that this clone may in fact be a member of the non-coding RNAs.

PTS542 was identified as a gene encoding Naked cuticle 2 (Nkd2), the transcript of which is detected in the middle PSM, and it seems that Mesp2 mutation does not affect the expression pattern of *nkd2*. *Naked cuticle* was first identified as a *Drosophila* segment polarity gene (Zeng et al., 2000) and mutation of this gene in the fly embryo causes similar phenotypes to excess Wg expression, indicating that Naked cuticle functions as an inhibitor of Wg signaling.

Since another Nkd protein in the mouse, Nkd1, can antagonize Wnt signaling in both cultured cells and in *Drosophila* embryos (Wharton et al., 2001), we determined whether *nkd1* is also expressed in the PSM and found that it exhibited an interesting expression pattern.

2.3. Mouse nkd1 mRNA oscillates in the PSM

nkd1 mRNA is first detected in the PSM and in the central nervous system of the 8.0 dpc embryo (Fig. 3A,B). In the 10.5 dpc embryo, *nkd1* expression is then observed in newly formed somites and in the neural tube, and was found to be maintained in the PSM (Fig. 3C). However, this expression pattern in the PSM varied among embryos and the signal was detected in either the middle of the PSM and tailbud (Fig. 3D) or in the more anterior PSM without tailbud (Fig. 3E). This suggests that the *nkd1* expression pattern changes in a short time in the PSM. To further analyze the precise transcriptional regulation of *nkd1*, we designed an RNA probe that was complementary to intronic sequences within the *nkd1* gene. Because this probe does not hybridize to mature spliced mRNA, we could therefore exclusively detect premature *nkd1* mRNA. Using the intronic RNA probe, we detected various expression patterns of *nkd1* in 11.5 dpc embryos (Fig. 3F–H), which could be categorized into three different phases, similar to other cyclic genes (Palmeirim et al., 1997; Bessho et al., 2001; Aulehla et al., 2003): Phase I: lower *nkd1* signal intensities in the tailbud. Phase II: *nkd1* transcripts are evident in the middle of the PSM in addition to the tailbud. Phase III: the *nkd1* signals shift more anteriorly. These results indicate that *nkd1* expression oscillates in the PSM during somitogenesis. However, another member of this family of genes, *nkd2* did not exhibit such periodic expression, although its expression was observed in the PSM (Fig. 2).

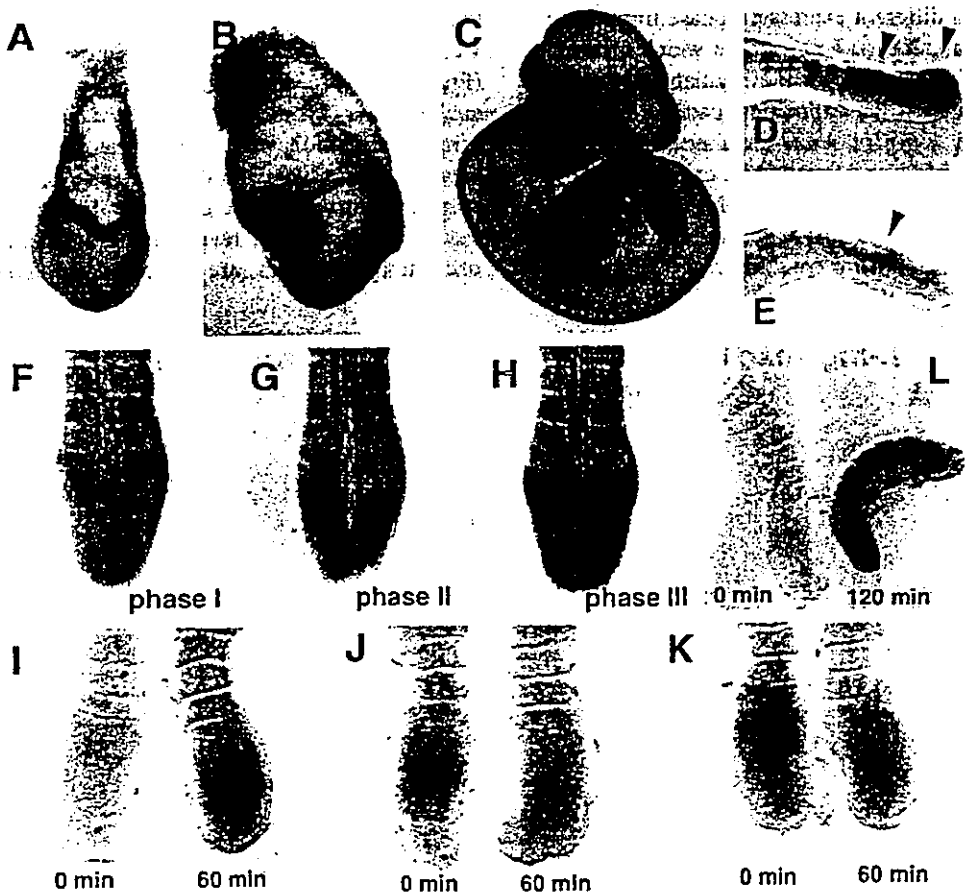

Fig. 3. Expression patterns of mouse *nkd1*. *nkd1* mRNA was detected with an exon probe at 7.5 dpc (A), 8.5 dpc (B), 10.5 dpc (C–E). *nkd1* transcripts are first detected in the central nervous system and in the PSM of 8.5 dpc embryos (B). In the 10.5 dpc embryo, *nkd1* expression is detected in the neural tube, dermomyotomes, somites and the PSM (C). Different expression patterns were detected using the exon probe (D,E). Arrowheads indicate signals in the PSM. (F–H) *nkd1* transcripts were detected using an intron probe in the tail region of 11.5 dpc embryos. Note that the expression is very weak in phase I (F), becomes stronger in the middle PSM in phase II (G) and is confined to the anterior PSM in phase III (H). (I–M) An embryo half culture experiment indicating the oscillation of *nkd1* expression. The 11.5 dpc embryo tails were cut into two halves at the midline. The left side was fixed immediately and the right side was fixed after 60 min (I–K) or 120 min (L) cultivation. Black and red arrowheads in (L) indicate segment border existed at 0 min and a newly formed border after 120 min, respectively. An intron probe was used for the ISH.

To further confirm the cyclic expression profile of *nkd1*, we performed in vitro cultures of bisected PSM, by fixing one half of the isolated tissue immediately and the additional half after a period of culturing. After 60 min, the expression patterns of *nkd1* in cultured PSM cells were altered from those of the uncultured portion (Fig. 3I–K). The change was most evident in the middle to anterior PSM, where the expression was seen to go from zero to strong levels and vice versa. After 120 min, the same pattern was observed which accompanied the formation of a new somite (Fig. 3L). These observations demonstrate that *nkd1* expression oscillates in the PSM during somitogenesis.

2.4. Comparisons of nkd1 expression patterns with other oscillatory genes

There are several genes that show periodic expression patterns during somitogenesis. The Notch-signaling related genes, *L-fng* and *hes7*, are transcribed with a similar oscillatory phase (Bessho et al., 2001), whereas the Wnt inhibitor *Axin2* has a different expression phase from these factors (Aulehla et al., 2003). To elucidate which of these signaling pathways is involved in the regulation of *nkd1* expression, we compared the expression patterns of *nkd1* with those of either *L-fng* or *Axin2* in dissected embryo halves. Surprisingly, *nkd1* was found to be expressed in the same phase as *L-fng* in the middle PSM (Fig. 4A–C), although its expression was not observed as a narrow band in the anterior PSM, as is the case for *L-fng* (Fig. 4B). These expression patterns are similar to those of the *hes7* transcripts detected with an intronic probe (Bessho et al., 2003). The oscillatory expression of both *L-fng* and of *hes7* itself is negatively controlled by Hes7 (Bessho et al., 2003). Thus, it appeared possible that *nkd1* expression would also be controlled by Hes7. On the other hand, the expression domains of *nkd1* and *Axin2* were obviously out of phase (Fig. 4D–F). For example, *Axin2* expression is not highly upregulated in the middle PSM where *nkd1* is strongly detected as phase II (Fig. 4E). *nkd1* expression is also detected as phase III in regions where *Axin2* expression is downregulated (Fig. 4F) and these spatial relationships resemble those of *Axin2* versus *L-fng* (Aulehla et al., 2003). These observations suggest that the oscillation of *nkd1* expression is regulated in a similar fashion to *L-fng*.

2.5. The oscillation of nkd1 expression is controlled by Hes7

To further confirm that the regulation of *nkd1* is under the control of the segmentation clock, via Notch signaling, we examined *nkd1* expression in the absence of Hes7 (Fig. 5A–C). In each of the Hes7-null embryos that we analyzed ($n=7$), the pattern of *nkd1* mRNA was similar. Strong expression was observed at the middle PSM, and weaker signals were observed in the remaining PSM. In comparison to wild-type embryos (Fig. 5D,E), it appeared that *nkd1* expression levels are upregulated and that its oscillatory patterns are arrested in Hes7 null-mice.

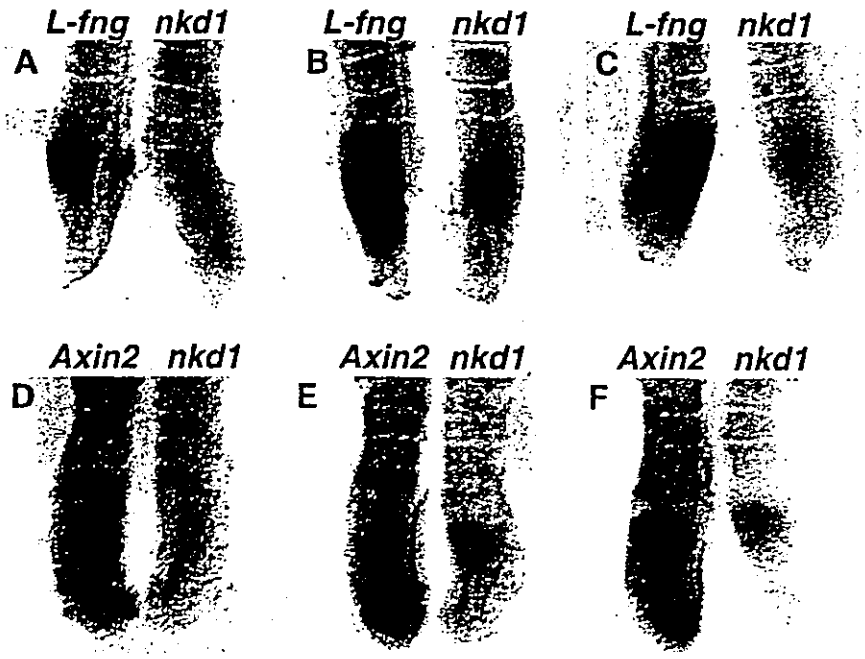

Fig. 4. Comparisons of the *nkd1* expression domains with the regions showing expression of other cyclic genes. (A–C) 11.5 dpc tail halves were stained with an *L-fng* probe (left) or an *nkd1* intron probe (right). The major expression domains overlapped with the exception of the anterior-most band of *L-fng* in B. (D–F) Embryo halves were stained with *Axin2* probe (left) or *nkd1* intron probe (right). The oscillatory phases of the expression patterns of *Axin2* and *nkd1* were found not to be synchronized.

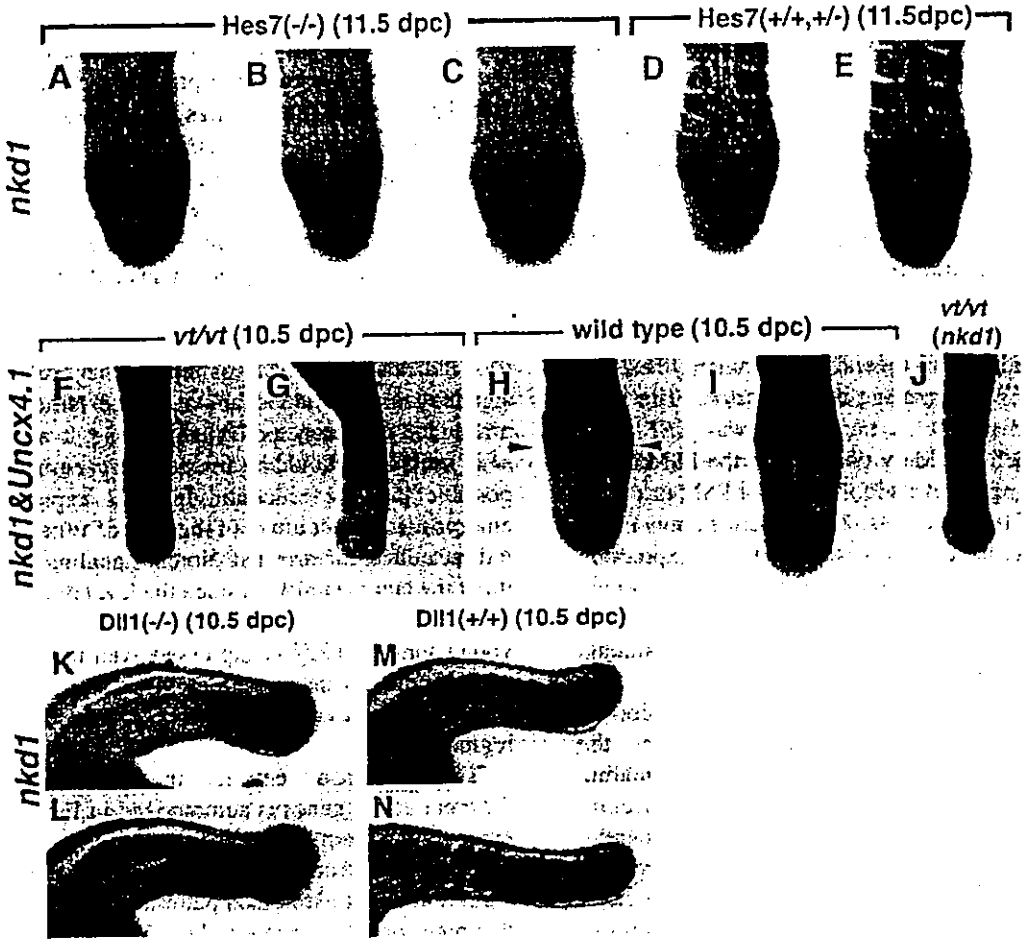

Fig. 5. *nkd1* oscillation is arrested in Hes7-null mice and its expression decreases in *vt/vt* mice but not in Dll1-null mice. (A–E) *nkd1* transcription was detected with an intron probe in either 11.5 dpc Hes7-null (A–C) or wild-type (D–E) littermate embryos. (F–I) *nkd1* expression in *vt/vt* and wild-type embryos was detected using an intron probe. *Uncx4.1* was used as an internal control. (J) *nkd1* probe alone was used in the *vt/vt* embryo. In the PSM of *vt/vt* embryos, *nkd1* mRNA is downregulated. The expression observed in the anterior PSM of wild-type embryo (arrowhead) corresponds to that of *nkd1* since *Uncx4.1* is expressed in the caudal portion of segmented somites. (K–N) *nkd1* expression in Dll1-null and wild-type embryos showing unaltered levels.

This suggests that the cyclic expression of *nkd1* depends on the negative regulation, either directly or indirectly, by the Hes7 transcription factor.

2.6. *nkd1 expression may be induced by Wnt signaling*

In fly embryos lacking *Wg*, *nkd* transcription initiates normally but is not subsequently maintained (Zeng et al., 2000). In human colon tumors, initiated by activated Wnt/β-catenin signaling, *hnkd* (*NKD1*) expression is elevated and experimental reduction of β-catenin leads to a decrease in *nkd1* mRNA (Yan et al., 2001b). These findings suggest that *nkd1* expression and/or maintenance depends on Wnt signaling. To determine whether Wnt signals affect *nkd1* expression during somitogenesis, we investigated *nkd1* expression in the *Wnt3a* hypomorphic mutant *vestigial tail* (*vt*) embryo. The *Wnt3a* coding sequence in the *vt* mouse is intact but its expression is markedly reduced in the tailbud from 9.5 dpc because of the mutation in the *Wnt3a* regulatory region (Greco et al., 1996). In *vt/vt* embryos ($n=4$), *nkd1* transcription is greatly reduced in the middle PSM and tailbud regions (Fig. 5F,G and data not shown) whereas expression levels in the neural tube and newly formed somites are normal (Fig. 5J). The expression levels of *L-fng*, however, are not altered in *vt/vt* embryos (Aulehla et al., 2003), although no oscillation is observed in these mutants. In the PSM, we have shown that *nkd1* mRNA oscillations are produced by a similar mechanism to *L-fng*, via negative regulation by Hes7. However, the induction and/or maintenance of *nkd1* transcription may require a different signal from *L-fng*, and we speculate that this is probably provided via Wnt3a. To further confirm this possibility, we have analyzed *nkd1* expression in Dll1-null embryos. As shown in (Fig. 5K–N), no reduction was observed, emphasizing that *nkd1* expression itself is independent of Notch signaling. However, no clear oscillation was observed, which also suggests Notch-signal dependent oscillation of *nkd1*.

Taken together, our data suggest that a possible crosstalk between the Notch and Wnt signaling mechanisms and that

their reciprocal regulation might therefore be important for generating the cyclic waves required for refining somitogenesis.

3. Discussion

We have employed a cDNA subtraction method to isolate previously uncharacterized genes that either function downstream of Mesp2 and/or are specifically expressed in the PSM. We successfully isolated several genes that are putatively involved in somitogenesis, and among these we identified several Wnt-signaling related factors. The most abundant gene identified in our screen was *LEF1*, the expression of which is widely observed in the PSM but is detected at its strongest levels in the anterior PSM just prior to segment border formation. *nkd2* is transcribed only in the middle PSM but we have demonstrated that *nkd1* expression oscillates in the PSM during somitogenesis. These facts may indicate that Wnt signaling has an important role in somitogenesis, consistent with previous findings (Aulehla et al., 2003).

It is generally believed that the spatial reiteration of somites is based on the periodicity generated by the molecular segmentation clock. Several Notch-signaling related factors are known components of the molecular clock during somitogenesis (Pourquié, 2001). Additionally, mice lacking Notch-related factors fail to form regular somites, providing strong evidence that the molecular clock organized by Notch signaling is required for formation of the reiterated somite structure. One of the best characterized molecular clock components is Hes7 (Bessho et al., 2003), the upregulation of which depends on Notch signaling. Both the auto-inhibitory activity and instability of the Hes7 protein are responsible for its oscillatory expression properties. Recently, it has been reported that *Axin2* expression also oscillates and that Wnt3a is required for the oscillation of Notch signaling in the PSM, which lead to a postulated link between Wnt/β-catenin signaling and the segmentation clock (Aulehla et al., 2003). However, the mechanisms underlying the regulation of these oscillations have not yet been determined.

We have found that *nkd1* expression exhibits oscillation with a similar phase to *L-fng* during somitogenesis, and that this oscillation is arrested and the expression is upregulated in Hes7-null embryos. These observations strongly suggest that *nkd1* transcription is suppressed by Hes7, with concomitant generation of its cyclic expression. To determine whether Hes7 can bind to the *nkd1* enhancer directly, we attempted to find a Hes7 binding site upstream of the *nkd1* gene. However, some of the 5′ flanking sequences of *nkd1* are absent from the databases and we have not yet fully sequenced the genomic region and so far not found any E-box or N-box sites within the available sequences. Future enhancer analysis of *nkd1* will therefore be necessary to properly determine this possibility.

In the embryo of the Wnt3a hypomorphic mutant, *vestigial tail*, the expression of *nkd1* is greatly reduced in the PSM. This suggests the possibility that Wnt signaling (mediated by Wnt3a) regulates the expression of *nkd1* in the PSM. This would be consistent with previous reports showing that the maintenance of *Drosophila nkd* expression depends on Wg function (Zeng et al., 2000) and that activated Wnt signals induce elevated *hnkd* expression levels in human colon tumors (Yan et al., 2001b). However, as the level of *nkd1* expression is increased and the oscillation of *nkd1* is disrupted in the Hes7-null mutant, this indicates that *nkd1* is under the control of Notch signaling as mentioned above. Since Notch signaling is arrested in the absence of Wnt signaling, it was feasible that *nkd1* oscillation would be arrested in *vt/vt* embryos. It is also possible that the reduction in *nkd1* expression in *vt/vt* embryos is a direct effect of the lack of Wnt signaling or an indirect effect of arrested Notch signaling. However, we think the latter is unlikely since the level of *nkd1* expression is unaltered in Dll1-null embryos. In the neural tube or in young somites, *nkd1* is expressed even in the *vt/vt* mutant, which indicates that additional Wnt signals or possibly a different pathway may regulate *nkd1* transcription in these regions.

The comparison between the expression domains of different cyclic genes is summarized in Fig. 6A. The *nkd1* expression pattern is similar to that of both *hes7* and *L-fng*, but is different from *Axin2*. The reason why *Axin2* and *nkd1* exhibit different expression patterns, irrespective of the fact that both appear to be induced by Wnt signaling, is currently unknown. One possibility is that *nkd1*, but not *Axin2*, oscillation is regulated by Notch signaling, which results in synchronization of *nkd1* oscillation with Notch signaling. In other words, the initial induction of *nkd1* might be induced by Wnt signaling but its regulation is under the control of Notch signaling. However, the expression patterns of Notch-related genes and *Axin2* are not completely mutually exclusive. They appear to be alternate in the tailbud region but they do align in the anterior PSM where *Mesp2* is expressed. Wnt3a appears to induce the expression of *Axin2* directly, but *Wnt3a* mRNA is detected only in the tailbud (Aulehla et al., 2003). Considering that Axin2 is expressed as a detectable band in the anterior PSM and that its expression is altered in Mesp2-null embryos, the expression pattern of *Axin2* may be regulated by Mesp2 in the anterior PSM. The direct targets of Mesp2 have not yet been characterized but many genes that are expressed in the anterior PSM are affected (downregulated or anteriorly expanded) by Mesp2, including *Notch1*, *Notch2*, *Fgfr1*, *Dll1*, *EphA4*, *Papc*, *Cer1* and *L-fng* (Saga et al., 1997; Takahashi et al., 2000; Nomura-Kitabayashi et al., 2002). Among them, EphA4 is implicated in segment border formation and ectodermal signaling is also required for *EphA4* induction (Schmidt et al., 2001), which may suggest that downstream genes of Wnt signal from the ectoderm might interact with Mesp2 to induce *EphA4*. *nkd1* is not

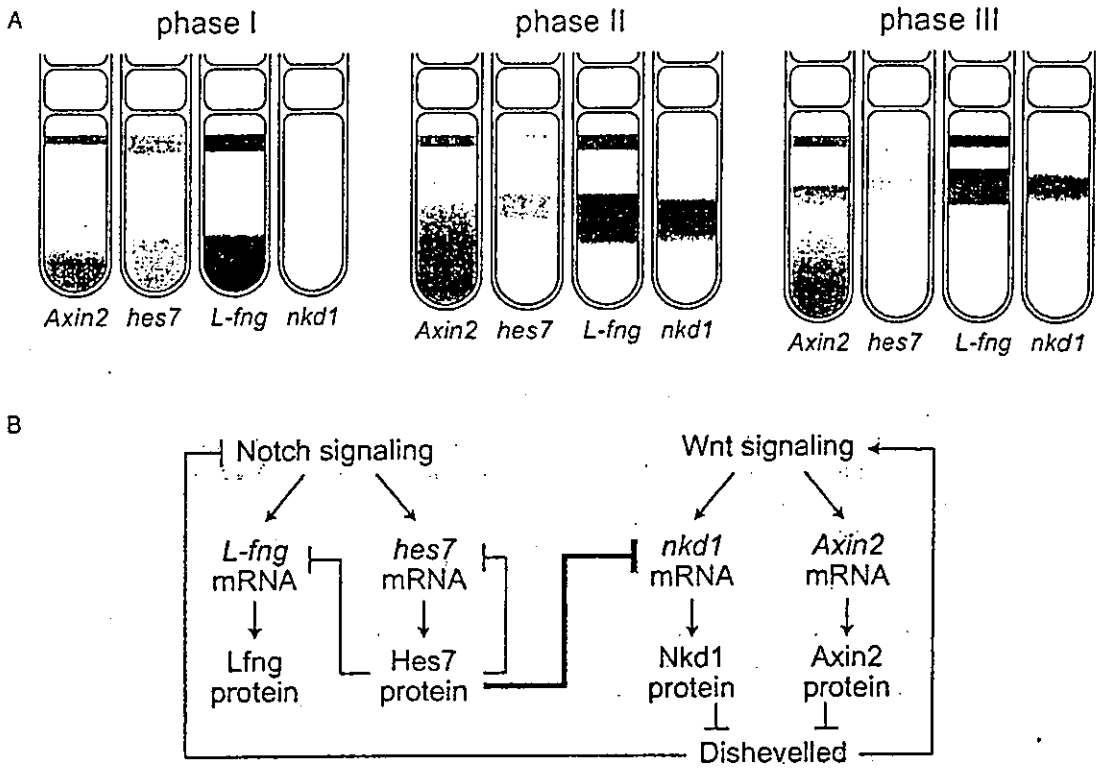

Fig. 6. (A) A schematic diagram of the expression patterns of oscillatory genes in the PSM of 11.5 dpc embryos. PhaseI: *Axin2*, *hes7* and *L-fng* show similar expression patterns in the tailbud and anterior PSM. *nkd1* transcription is greatly downregulated in this phase. PhaseII: The expression domain of *Axin2* is more extensive in the tailbud region. *hes7*, *L-fng* and *nkd1* are all expressed in the same region of the middle PSM, whereas *nkd1* is not detected in the anterior PSM in a band-like pattern. PhaseIII: *Axin2* expression is downregulated in the middle PSM. Around S-1, the expression of all four genes overlaps. (B) Possible interactions between Notch and Wnt signaling. Our findings are integrated into the previously proposed schemes of Bessho et al. (2003) and Aulehla et al. (2003). We propose that Wnt signaling may be regulated by Notch signals via the transcriptional regulation of *nkd1* by Hes7. It has been reported previously that Wnt signaling may regulate Notch signaling via NICD inhibition by Dishevelled (Axelrod et al., 1996).

expressed in the anterior PSM and its expression is regulated by Hes7, but not by Mesp2 (data not shown). There may be different gene regulatory mechanisms along the AP axis in the PSM, where the cyclic expression in the posterior PSM must be regulated by a clock mechanism, but expression in the anterior PSM may also be regulated by a different mechanism under the control of Mesp2. The link between these two mechanisms is currently unknown but the clock mechanism which is operated by both Wnt and Notch signaling may affect Mesp2 regulation.

nkd is a *Drosophila* segment polarity gene that encodes an antagonist of the Wnt signal, Wingless. It is known that mouse Nkd1 directly binds to Dishevelled (Dvl) (Wharton et al., 2001) and that Nkd1 antagonizes Wnt signaling in both *Xenopus* (Yan et al., 2001a) and *Drosophila* (Wharton et al., 2001) embryos. Thus, it is possible that the Nkd1 protein also functions as an antagonist of Wnt signaling in the PSM. Of great interest, therefore, is the exact function of Nkd1 during somitogenesis. Using luciferase reporter assays, it has previously been demonstrated that *Axin2* is directly upregulated by Wnt/β-catenin signaling (Aulehla et al., 2003). One possibility, therefore, for the function of Nkd1 is that, in mouse, it suppresses the transcription of *Axin2* by antagonizing the Wnt signals, and hence, Nkd1 oscillations may contribute to the oscillatory expression of *Axin2*. To further address this question, it will be necessary to analyze the distribution of the Nkd1 protein and examine whether it has a sufficiently high turnover to generate such oscillatory expression patterns. However, both Axin and Nkd1 have been demonstrated to bind Dvl via its PDZ domain (Li et al., 1999; Seidensticker and Behrens, 2000; Yan et al., 2001a; Wharton et al., 2001). Hence, if Axin2 can bind Dvl with a similar affinity as Axin, it may compete with Nkd1 for Dvl binding to initiate distinct functions. Alternatively, they may work co-operatively to suppress Dvl. The binding to Dvl not only affects Wnt signaling but also may affect Notch signaling since it has already been shown to bind the processed form of Notch receptor (NICD) (Axelrod et al., 1996). It has also been reported that Dvl1/Dvl2 double knockout embryos exhibit defects in somite segmentation (Hamblet et al., 2002), which may suggest that regulation of Wnt signaling via Axin2 and /or Nkd1 is involved in segmental patterning. The link between Wnt and Notch signaling remains one of the central unsolved mechanisms underlying both the generation and regulation of the segmentation clock. Since *nkd1* oscillation is

disrupted in Hes7-null mutants, there may be a negative feed-back loop between the Notch and Wnt signaling pathways and it is likely that their interaction is essential for the establishment of the molecular clock required for accurate somitogenesis (Fig. 6B).

4. Experimental procedures

4.1. Experimental animals

Heterozygous Mesp2-mutant (*Mesp2*$^{+/-}$) mice were intercrossed to obtain either homozygous, heterozygous or wild-type embryos in the same litter. The appearance of vaginal plugs was designated as embryonic day 0.5 (dpc). Homozygous Mesp2-null embryos were identified by a no segmentation phenotype, as described previously (Saga et al., 1997). Hes7-knockout mice and Dll1-knockout mice were kindly provided by Yasumasa Bessho (Kyoto Univ. Japan) and Achime Gosller (Hanover Univ. Germany), respectively. Samples of *vt/vt* embryos were provided by Shinji Takada (National Institute for Basic Biology, Japan).

4.2. Preparation of subtractive cDNA libraries

As shown in Fig. 1, total RNA isolates were prepared from two pieces of the dissected portions of either wild-type (WP: PSM of wild-type and WS: somite region of wild-type) or homozygous (HPS: PSM of Mesp2-null) 11.5 dpc embryos using Isogen (Nippon Gene, Japan). We utilized the subtractive hybridization method of Kaneko-Ishino et al. (1995) with slight modifications. Briefly, to generate tester cDNAs for subtraction, cDNAs were synthesized and amplified with the Smart cDNA Amplification Kit (Clontech, USA), whereas the driver cDNAs were generated using a cDNA Synthesis Kit (TaKaRa, Japan). Amplification of driver cDNAs was performed using a ligated linker (P-linker). A biotinylated P-primer, complementary to the P-linker, was used for the subsequent PCR (Kaneko-Ishino et al., 1995).

PCR primer 5′-AAGCAGTGGTAACAACGCAGAGT-3′.
P-linker 5′-GATTACTCGAGACTAATATC-3′;
5′-pGATATTAGTCTCGAGTA-3′.

We constructed two libraries; one generated by subtraction between [WP] (tester) and [WS] (driver) to enrich for PSM genes, and a second synthesized by subtraction between [WP] (tester) and [HPS] (driver) to enrich for possible Mesp2 downstream genes. Tester cDNA samples (60 ng) were hybridized to biotinylated driver cDNAs (1.2 μg) (the ratio was increased to 1:100 in the case of the second and third subtractions). After ethanol precipitation, total cDNAs were subjected to absorption by 4 mg of Dynabeads M-280 conjugated to streptavidin (Dynal). The remaining cDNAs were amplified by PCR. One half of each sample was used for the subsequent subtraction steps, and the cDNA isolates that were obtained after three consecutive subtractions and PCR amplifications were cloned into the pCRII vector using a TA Cloning Kit (Invitrogen). We designated these subtractive libraries as the PTS library for [WP] and [WS], and as the ST library for [WP] and [HPS].

4.3. Sequencing and computer analysis

cDNA clones that were randomly selected from both of the subtractive libraries that we generated, 406 and 636 clones from PTS and ST, respectively, were partially sequenced and analyzed using the BLAST program through the National Library of Medicine and Celera databases. Only novel clones were further screened by ISH. The numbers of selected clones were 251 and 280, for PTS and ST, respectively.

4.4. Screening by in situ hybridization

The basic method used for whole mount ISH has been described previously by our laboratory (Saga et al., 1996), although for this study automated ISH was employed (InsituPro, M&S Instruments Trading Inc. Japan). The tail regions, containing both somite and PSM of 11.5 dpc embryos, were used in these analyses. RNA probes were generated by transcription, with either T7 RNA polymerase or SP6 RNA polymerase, of template DNAs prepared by PCR using M13 specific sites within the vector. M13 reverse primer: 5′-CAGGAAACAGCTATGAC-3′; M13 forward primer: 5′-GTAAAACGACGGCCAG-3′.

4.5. Whole-mount in situ hybridization probes

A BamHI-PstI 429 bp fragment of *nkd1* cDNA was used as an *nkd1* exon probe. As *nkd1* intron probes, we utilized a mixture of two genomic fragments; the XbaI 1.3 kb fragment in intron 4 and the NcoI 1.4 kb fragment in intron 6. For *Axin2* hybridization, we amplified a 1360 bp PCR fragment from the coding region of this gene from a PSM cDNA library (Ohara et al., 2002) using the forward primer 5′-GTCTGGAGGAGCGGCTGCAGCAGATCCG-3′ and reverse primer 5′-CAAGGCTCAGTCGATCCTCTC-CACTTTGC-3′.

4.6. In vitro explant cultures

In vitro explant culture was performed as previously described (Takahashi et al., 2000). The tail regions of ICR embryos (11.5 dpc) were bisected at the midline with either a tungsten or ground sewing needle. One half was fixed immediately and the other was cultured for either 60 or 120 min. After culturing, specimens were fixed and used for subsequent ISH analysis.

Acknowledgements

We thank Yasumasa Bessho for providing the Hes-7 knockout mouse and Shinji Takada for donating the vt/vt embryos. We also thank Mariko Ikumi, Izumi Uehara and Eriko Ikeno for general technical assistance. This work was supported by Grants-in-Aid for Science Research on Priority Areas (B), the Organized Research Combination System and National BioResource Project of the Ministry of Education, Culture, Sports, Science and Technology, Japan.

References

Aulehla, A., Wehrle, C., Brand-Saberi, B., Kemler, R., Gossler, A., Kanzler, B., Herrmann, B.G., 2003. Wnt3a plays a major role in the segmentation clock controlling somitogenesis. Dev. Cell 4, 395–406.

Axelrod, J.D., Matsuno, K., Artavanis-Tsakonas, S., Perrimon, N., 1996. Interaction between Wingless and Notch signaling pathways mediated by dishevelled. Science 271, 1826–1832.

Behrens, J., Jerchow, B., Würtele, M., Grimm, J., Asbrand, C., Wirtz, R., et al., 1998. Functional interaction of an axin homolog, conductin, with β-catenin, APC, and GSK3β. Science 280, 596–599.

Bessho, Y., Sakata, R., Komatsu, S., Shiota, K., Yamada, S., Kageyama, R., 2001. Dynamic expression and essential functions of Hes7 in somite segmentation. Genes Dev. 15, 2642–2647.

Bessho, Y., Hirata, H., Masamizu, Y., Kageyama, R., 2003. Periodic repression by the bHLH factor Hes7 is an essential mechanism for the somite segmentation clock. Genes Dev. 17, 1451–1456.

Dubrulle, J., McGrew, M.J., Pourquie, O., 2001. FGF signaling controls somite boundary position and regulates segmentation clock control of spatiotemporal Hox gene activation. Cell 106, 219–232.

Greco, T.L., Takada, S., Newhouse, M.M., McMahon, A.P., Camper, S.A., 1996. Analysis of the vestigial tail mutation demonstrates that Wnt-3a gene dosage regulates mouse axial development. Genes Dev. 10, 313–324.

Hamblet, N.S., Lijam, N., Ruiz-Lozano, P., Wang, J., Yang, Y., Luo, Z., et al., 2002. Dishevelled 2 is essential for cardiac outflow tract development, somite segmentation and neural tube closure. Development 129, 5827–5838.

Hsu, S., Galceran, J., Grosschedl, R., 1998. Modulation of transcriptional regulation by LEF-1 in response to Wnt-1 signaling and association with β-catenin. Mol. Cell Biol. 18, 4807–4818.

Kaneko-Ishino, T., Kuroiwa, Y., Miyoshi, N., Kohda, T., Suzuki, R., Yokoyama, M., et al., 1995. Peg1/Mest imprinted gene on chromosome 6 identified by cDNA subtraction hybridization. Nature Genet. 11, 52–60.

Li, L., Yuan, H., Weaver, C.D., Mao, J., Farr III., G.H., Sussman, D.J., et al., 1999. Axin and Frat1 interact with dvl and GSK, bridging Dvl to GSK in Wnt-mediated regulation of LEF-1. Eur. Mol. Biol. Org. J. 18, 4233–4240.

Liu, Y., Jiang, H., Crawford, H.C., Hogan, B.L., 2003. Role for ETS domain transcription factors Pea3/Erm in mouse lung development. Dev. Biol. 261, 10–24.

Nomura-Kitabayashi, A., Takahashi, Y., Kitajima, S., Inoue, T., Takeda, H., Saga, Y., 2002. Hypomorphic Mesp allele distinguishes establishment of rostrocaudal polarity and segment border formation in somitogenesis. Development 129, 2473–2481.

Ohara, O., Nagase, T., Mitsui, G., Kohga, H., Kikuno, R., Hiraoka, S., et al., 2002. Characterization of size-fractionated cDNA libraries generated by the in vitro recombination-assisted method. DNA Res. 9, 47–57.

Palmeirim, I., Henrique, D., Ish-Horowicz, D., Pourquié, O., 1997. Avian hairy gene expression identifies a molecular clock linked to vertebrate segmentation and somitogenesis. Cell 91, 639–648.

Porfiri, E., Rubinfeld, B., Albert, I., Hovanes, K., Waterman, M., Polakis, P., 1997. Induction of a β-catenin-LEF-1 complex by wnt-1 and transforming mutants of β-catenin. Oncogene 15, 2833–2839.

Pourquié, O., 2001. Vertebrate somitogenesis. Annu. Rev. Cell Dev. Biol. 17, 311–350.

Rasmussen, J.T., Deardorff, M.A., Tan, C., Rao, M.S., Vetter, M.L., 2001. Regulation of eye development by frizzled signaling in Xenopus. Proc. Natl Acad. Sci. USA 98, 3861–3866.

Ristevski, S., Tam, P.P., Hertzog, P.J., Kola, I., 2002. Ets2 is expressed during morphogenesis of the somite and limb in the mouse embryo. Mech Dev. 116, 165–168.

Saga, Y., Hata, N., Kobayashi, S., Magnuson, T., Seldin, M., Taketo, M.M., 1996. MesP1: a novel basic helix-loop-helix protein expressed in the nascent mesodermal cells during mouse gastrulation. Development 122, 2769–2778.

Saga, Y., Hata, N., Koseki, H., Taketo, M.M., 1997. Mesp2: a novel mouse gene expressed in the presegmented mesoderm and essential for segmentation initiation. Genes Dev. 11, 1827–1839.

Sawada, A., Shinya, M., Jiang, Y.J., Kawakami, A., Kuroiwa, A., Takeda, H., 2001. Fgf/MAPK signalling is a crucial positional cue in somite boundary formation. Development 128, 4873–4880.

Schmidt, C., Christ, B., Maden, M., Brand-Saberi, B., Patel, K., 2001. Regulation of Epha4 expression in paraxial and lateral plate mesoderm by ectoderm-derived signals. Dev. Dyn. 220, 377–386.

Seidensticker, M.J., Behrens, J., 2000. Biochemical interactions in the wnt pathway. Biochem. Biophys. Acta 1495, 168–182.

Takada, S., Stark, K.L., Shea, M.J., Vassileva, G., McMahon, J.A., McMahon, A.P., 1994. Wnt-3a regulates somite and tailbud formation in the mouse embryo. Genes Dev. 8, 174–189.

Takahashi, Y., Koizumi, K., Takagi, A., Kitajima, S., Inoue, T., Koseki, H., Saga, Y., 2000. Mesp2 initiates somite segmentation through the Notch signalling pathway. Nature Genet. 25, 390–396.

Takahashi, Y., Inoue, T., Gossler, A., Saga, Y., 2003. Feedback loops comprising Dll1, Dll3 and Mesp2, and differential involvement of Psen1 are essential for rostrocaudal patterning of somites. Development 18, 4259–4268.

Tan, C., Deardorff, M.A., Saint-Jeannet, J.P., Yang, J., Arzoumanian, A., Klein, P.S., 2001. Kermit, a frizzeled interacting protein, regulates frizzeled 3 signaling in neural crest development. Development 128, 3665–3674.

Wharton Jr., K.A., Zimmermann, G., Rousset, R., Scott, M.P., 2001. Vertebrate proteins related to Drosophila Naked Cuticle bind Dishevelled and antagonize Wnt signaling. Dev. Biol. 234, 93–106.

Yamamoto, H., Flannery, M.L., Kupriyanov, S., Pearce, J., McKercher, S.R., Henkel, G.W., et al., 1998. Defective trophoblast function in mice with a targeted mutation of Ets2. Genes Dev. 12, 1315–1326.

Yan, D., Wallingford, J.B., Sun, T.Q., Nelson, A.M., Sakanaka, C., Reinhard, C., et al., 2001a. Cell autonomous regulation of multiple Dishevelled-dependent pathways by mammalian Nkd. Proc. Natl Acad. Sci. USA 98, 3802–3807.

Yan, D., Wiesmann, M., Rohan, M., Chan, V., Jefferson, A.B., Guo, L., et al., 2001b. Elevated expression of axin2 and hnkd mRNA provides evidence that Wnt/β-catenin signaling is activated in human colon tumors. Proc. Natl Acad. Sci. USA 98, 14973–14978.

Zeng, W., Wharton Jr., K.A., Mack, J.A., Wang, K., Gadbaw, M., Suyama, K., et al., 2000. Naked cuticle encodes an inducible antagonist of Wnt signalling. Nature 403, 789–795.

Toxicologic Pathology, 32(Suppl. 2):12–16, 2004

ISSN: 0192-6233 print / 1533-1601 online
DOI: 10.1080/01926230490451725

Mechanism of Benzene-Induced Hematotoxicity and Leukemogenicity: Current Review with Implication of Microarray Analyses

YOKO HIRABAYASHI,[1] BYUNG-IL YOON,[1,2] GUANG-XUN LI,[1] JUN KANNO,[1] AND TOHRU INOUE[3]

[1]*Division of Cellular and Molecular Toxicology, National Institute of Health Sciences, Tokyo 158-8501, Japan*
[2]*Department of Veterinary Medicine, Kangwon National University, Kangwon 200-701, Republic of Korea, Seoul National University, Seoul 151-742, Republic of Korea, and*
[3]*Biological Safety and Research Center, National Institute of Health Sciences, Tokyo 158-8501, Japan*

ABSTRACT

Benzene is a potent human leukemogen but the mechanism underlying benzene-induced leukemia remains an enigma due to a number of questions regarding the requirement of extraordinarily long exposure, a relatively low incidence of leukemia for genotoxicity of metabolites and a narrow dose range for leukemogenicity over marrow aplasia (overdoses tend to result in marrow aplasia). Moreover, there were previous controversies as to whether the cell cycle is upregulated or suppressed by the benzene exposure. Subsequently, it was found that the cell cycle is suppressed, but how leukemia develops under such suppression of hemopoiesis remains to be clarified. These questions were fortunately resolved with much effort. Benzene exposure was found to induce the expression of p21, an interlocking counterdevice for cell cycle: due to *p53* upregulation, thereby inducing the immediate suppression of the kinetics of hemopoietic progenitors followed by the prominent suppression of hemopoiesis. Intermittent benzene exposure (i.e., cessation of exposure during weekends, for example) allowed an immediate recovery from marrow suppression after terminating exposure, which induced continuous oscillatory changes in marrow hemopoiesis. Benzene-induced leukemia was chiefly due to such an oscillatory change in hemopoiesis, which epigenetically developed leukemia more than 1 year later. The mechanisms of benzene-induced leukemogenicity seem to differ between wild-type mice and mice lacking *p53*. For *p53* knockout mice, DNA damage such as weak mutagenicity or chromosomal damage was retained, and such damage induced consequent activation of proto-oncogenes and related genes, which led cells to undergo further neoplastic changes. In contrast, for wild-type mice carrying the *p53* gene, a marked oscillatory change in the cell cycle of the stem cell compartment seems to be important. Compatible and discriminative gene expression profiling between the *p53* knockout mice and wild-type mice was observed after benzene exposure by microarray analyses.

Keywords. Benzene; hematotoxicity; leukemogenicity; gene chip array; BUUV method; *p53*-KO; AhR-KO; hemopoietic progenitor cells.

INTRODUCTION

The mechanism of benzene-induced leukemia had long been an enigma until recently, when the unique cell kinetics of stem/progenitor cells during benzene exposure was elucidated. Leukemia induction by benzene inhalation was first reported in 1897, when Le Noire described multiple cases of leukemia among Parisian cobblers (Le Noir and Claude, 1897). However, the experimental induction of leukemia by benzene exposure was first reported about 20 years ago by Snyder et al. (1980) and our group (Cronkite et al., 1984, 1989). Recently, we demonstrated marked oscillatory changes in peripheral blood and bone marrow (BM)[1] cellularities during and following benzene inhalation, preceding the development of leukemia by about 1 year (Hirabayashi et al., 1998; Kawasaki et al., 2001; Yoon et al., 2001).

Address correspondence to: Tohru Inoue, Center for Biological Safety and Research, National Institute of Health Sciences, 1-18-1 Kamiyohga, Setagayaku, Tokyo 158-8501, Japan; e-mail: tohru@nihs.go.jp

[1]Abbreviations: BM, bone marrow; KO, knockout; UV, ultraviolet; BUUV, incorporation of bromodeoxyuridine followed by ultraviolet-light cytocide to evaluate the hemopoietic stem/progenitor cell kinetics in vivo; AhR, aryl hydrocarbon receptor; $AhR^{+/+}$, AhR wild-type; $AhR^{+/-}$, AhR heterozygous-deficient; $AhR^{-/-}$, AhR homozygous-deficient; CFU-GM, granulo-macrophage colony forming unit; CYP, cytochrome P450; FGF, fibroblast growth factor; TGF, tumor growth factor; I.V., intravenous; I.P., intraperitoneal; aft, after; dur, during; expos, exposure.

Benzene-induced leukemia is unique in that it has been associated only with a weak mutagenicity in the benzene metabolites, phenol and hydroquinone. Another interesting observation is the controversial experimental data concerning the level of actively cycling hematopoietic cells following benzene exposure. While all researchers observed a decrease in peripheral blood and BM cellularities, some observed a suppression of the cell cycle of BM, as measured by tritiated thymidine incorporation (Moeschlin and Speck, 1967), whereas others observed a marked increase in the number of cycling stem/progenitor cells in BM and peripheral blood (Table 1). Careful analysis of these apparently conflicting data revealed an enhancement of the cell cycle occurring at least 2 hours after the termination of benzene exposure. Thus, the higher tritiated thymidine incorporation documented by Cronkite et al. (1982) 18 hours after the termination of benzene exposure probably reflects a recovery phase. Based on these findings, we conducted a series of studies since 1997 to elucidate the leukemogenic effect of benzene in wild-type mice.

The *p53*-knockout (KO) mouse (Tsukada et al., 1993) showed further unique characteristics of benzene-induced leukemia. Using *p53*-KO mouse, we confirmed that benzene has a moderate genotoxic effect, as measured by the micronucleus test performed 4 weeks after the initiation of benzene inhalation (Kawasaki et al., 2001; Li et al., 2003). Moreover, *p53*-deficient mice manifest increased susceptibility to

TABLE 1.—Summary of the results the hemopoietic stem/progenitor cell kinetics during and after benzene exposure by tritiated thymidine (^{3}H-TdR) cytocide assay.

				Evaluation cell and assay methods					
		Cellularity		BM cells			CFU		
Year	Reference	Blood	BM	Kinetics	Labeling*,1	Label point	Kinetics	Labeling	Label point
1967	Moeschlin and Speck	↓	↓	↓	In vivo	At pancytopenia	—	—	—
1979	Irons et al.	↓	↓	↑	In vivo[2]	6 days aft. expos-IP	—	—	—
1982	Cronkite et al.	↓	↓	—	—	—	↑	In vitro	18 h aft. expos.
1998	Lee et al.	↓	↓	↓	In vivo[3]	30 min aft. single IP	—	—	—
		↓	↓	↓	In vitro	Dur. and aft. expos.	—	—	—
1997	Farris et al.	↓	↓	→↓	In vivo[4]	Soon aft. expos.	↑	In vitro	2 h aft. expos.

1. ^{3}H-TdR was injected intravenous (IV) at in vivo labeling except indications.
2. ^{3}H-TdR was injected intraperitoneal (IP) 6 days after cessation of benzene.
3. Benzene was treated single IP, and ^{3}H-TdR label was starting 30 minutes after benzene treatment.
4. Instead of ^{3}H-TdR, BrdUrd was used for assay.

benzene-induced leukemogenicity (Kawasaki et al., 2001). Similar findings with regard to increased leukemogenicity following benzene exposure have been documented by French et al. of the National Institute of Environmental Health Sciences (French et al., 2001). Contrary to the result in *p53*-KO mice, benzene-induced leukemia had not been detected in earlier studies in wild-type mice because its manifestations had been masked either by pancytopenia due to severe myelosuppression or by the use of a benzene dose too low to induce pancytopenia or leukemia (Kawasaki et al., 2001). Aryl hydrocarbon receptor (AhR)-KO mice (Mimura et al., 1997) also elucidated the characteristic underlying mechanism of benzene-induced hematotoxicity (Yoon et al., 2002).

In the mechanism underlying benzene toxicity in BM tissue analyzed using a microarray system, various signaling pathways have been suggested to be implicated including cell cycle regulation, DNA-damage/repair-related genes, oxidative-stress-related genes, growth-factor-related genes, oncogenes, and hemopoiesis-related genes in general (Yoon et al., 2003).

Oscillatory Changes in Bone Marrow Cellularity in Wild-Type Mice

BM cellularity decreases markedly during benzene inhalation but recovers rapidly following the termination of benzene exposure (Yoon et al., 2001). The oscillatory nature of the resultant curve is comparable to the response reported by Cronkite et al. (1984, 1989), and suggests that benzene does not only induce BM cell suppression but also activates cell-cycle-regulating genes, resulting in compensatory myelopoiesis.

We used the BUUV (bromodeoxyuridine + UV exposure) method to study stem/progenitor cell kinetics during or after benzene exposure (Hirabayashi et al., 1998; Yoon et al., 2001). Using this method, we were able to measure the labeling rate, cycling fraction of clonogenic progenitor cells, and other cell cycle parameters. Interestingly, the cycling fraction of stem/progenitor cells was found not to turn into active hematopoiesis but to remain low during benzene inhalation. Furthermore, rapid recovery was observed after benzene inhalation was terminated (Figure 1). However, although the exact mechanism of this phenomenon is not yet known, we found the evidence that the cycling fraction depression may be mediated in part by the suppression of stem/progenitor cell cycling per se, owing to the *p53*-dependent upregulation of p21 (Yoon et al., 2001). Thus, the mechanism of benzene-induced leukemia in the wild-type mice may be due to continuous oscillatory changes in hemopoiesis during and after the benzene exposure, which leads to genetic instability followed by the consequent epigenetic leukemogenicity.

p53-Deficient Mice Develop Leukemia by Different Mechanisms

Leukemogenicity induced in *p53*-KO mice, because of the lack of the *p53* gene, results in the noninduction of p21 expression even during the benzene exposure, with subsequent insufficient DNA repair and accumulation of DNA damage. These pathways are shown in Figure 2 for benzene-induced possible toxicological changes in both wild-type and *p53*-KO mice. In *p53*-KO mice, cell cycle suppression, DNA repair, and apoptosis of damaged cells, which, in general, occur in the wild-type mice after benzene exposure, are all suppressed. This is much more likely genotoxic leukemogenesis, in which reactive oxygen species, dysfunction of topoisomerase, and covalent binding of adduct formation to DNA,

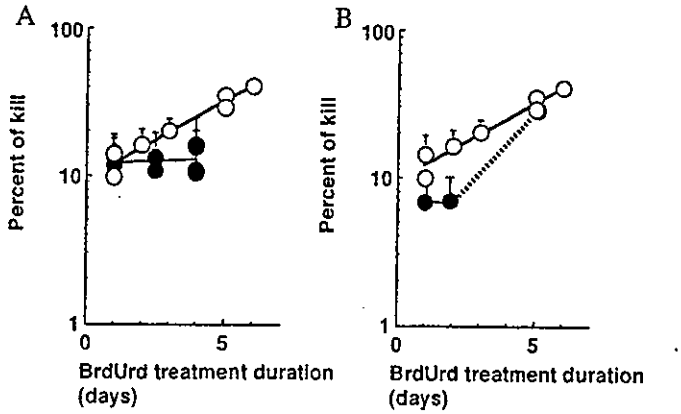

FIGURE 1.—Hemopoietic progenitor cell (CFU-GM) kinetics during (A) and after (B) benzene inhalation. Open circle: sham; Closed circle: during or after inhalation of 300 ppm benzene, 6 h/day, 5 days/week ×2 weeks. (A) For the benzene-treated group, all the mice were sacrificed just after the 5th day of the 2nd week of benzene-inhalation. The osmotic minipump filled with BrdUrd was implanted into donor mice day(s) before sacrificing as indicated on the abscissa. (B) For the benzene-treated group, the BrdUrd-pump was implanted into donor mice after the 5th day of the 2nd week of benzene-inhalation and sacrificed on the day as indicated on the abscissa. Each point represents at least 2 mice as a donor for the CFU-GM assay, and colony assays were performed in triplicate.

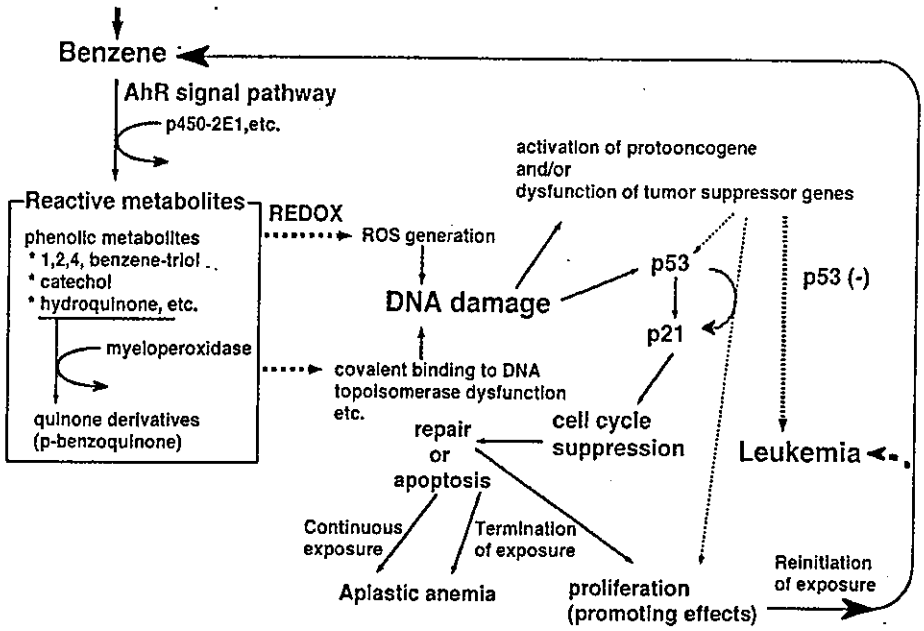

FIGURE 2.—Benzene metabolism and possible mechanism of benzene-induced leukemogenesis.

all synergistically participate in further leukemogenic development without repairing the system (see Figure 2). Thus, leukemogenicity seems to be clearly different between the mice carrying wild-type *p53* and the mice lacking *p53* (Yoon et al., 2001; Hirabayashi et al., 2002).

ARYLHYDROCARBON-RECEPTOR-MEDIATED BENZENE METABOLISM

We investigated the involvement of the aryl hydrocarbon receptor (AhR), a ligand-activated basic helix-loop-helix transcription factor, in hematotoxicity using AhR wild-type ($AhR^{+/+}$), heterozygous-KO ($AhR^{+/-}$) and homozygous-KO ($AhR^{-/-}$) male mice (Mimura et al., 1997; Yoon et al., 2002). Following a 2-week inhalation of benzene at 300 ppm, we evaluated the changes in cellularity of the peripheral blood and BM, and the levels of granulocyte-macrophage colony-forming units (CFU-GM) in the BM (Figure 3). The expression of the cyclin-dependent kinase inhibitor, p21, in BM cells and cytochrome P450 (CYP) 2E1 in hepatic tissues were evaluated by Western blot analysis after benzene exposure. Our results clearly showed that $AhR^{-/-}$ mice are much more resistant to the benzene-induced hematotoxicity than $AhR^{+/+}$ wild-type mice. No changes in p21 expression level by BM cells were detected in $AhR^{-/-}$ mice, whereas a marked up-regulation of p21 expression by BM cells was observed in $AhR^{+/+}$ mice. This finding is a further proof of the resistance of $AhR^{-/-}$ mice to benzene-induced hematotoxicity. The benzene resistance of $AhR^{-/-}$ mice was abrogated by exposure to a combination of 2 major metabolites, phenol and hydroquinone, strongly supporting the notion that AhR participates in benzene metabolism. CYP species involved in such metabolism are under investigation. The results obtained imply that pollutants that react with AhR confer marked susceptibility to benzene-induced hematotoxicity.

IMPLICATION OF MICROARRAY ANALYSIS

In the mechanism underlying benzene toxicity in BM tissue, various signaling pathways have been suggested to be implicated including metabolism, genotoxicity, cell cycle regulation, and apoptosis (Table 2). Our microarray analysis

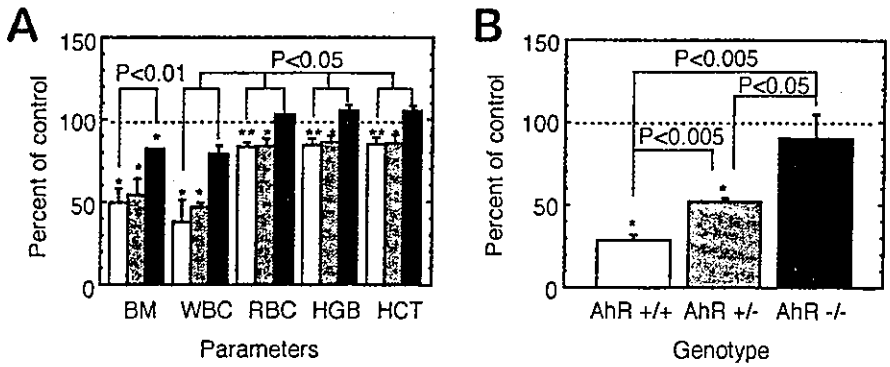

FIGURE 3.—Changes in peripheral blood parameters and BM cellularity (A) and CFU-GM per 2 femurs (B) in the AhR wild-type ($AhR^{+/+}$:open bar), heterozygous-KO ($AhR^{+/-}$:shaded bar) and homozygous-KO mice ($AhR^{-/-}$:closed bar) exposed to 300 ppm benzene for 2 weeks. The mean BM cellularities for the $AhR^{+/+}$, $AhR^{+/-}$, and $AhR^{-/-}$ mice were 4.8, 5.6, and 4.8 × 10^7/2 femurs, respectively, and the mean numbers of CFU-GM's per 8 × 10^4 BM cells was 79, 78, and 72, respectively. *, **: Significantly different from each corresponding control group at $p < 0.05$ and $p < 0.01$, respectively.

TABLE 2.—Reported genes whose expression changed during and/or after benzene inhalation.

Category	Gene name	Reference
Metabolic enzyme	CYP 2E1	Zhang et al., 2002
	Myeloperoxidase	Schattenberg et al., 1994
Cell cycle	*p53*	Boley et al., 2002
	p21 (waf 1)	
	Cyclin G	
	Gadd 45	
Apoptosis	Bax-alpha	Boley et al., 2002
Oncogene	c-fos	Ho and Witz, 1997

elucidated the up- or downregulation of genes functioning after 2-week exposure to 300 ppm benzene (Table 3): First, among cell-cycle-related genes, in addition to *p53* and p21 which are known to be upregulated to various extents depending upon the time course and the detection methods, Rb-related genes, such as the Rb-related protein p130 and the Rb-binding protein p48 are significantly upregulated; furthermore, elongation factor 1-delta shows a high expression level associated with the G2/M cell cycle checkpoint; vice versa, a significant downregulation of cyclin D1 and BimB is also recognized. Less significant changes in expression of cyclin G and Gadd45 are noted as previously reported. Second, among DNA-damage/repair-related genes, those encoding ADP-ribosylation factor-like protein 1 and Rad51 are significantly upregulated. The altered expression of other genes in the same category such as Metaxin, ERCC-3, and the DTR111 precursor are also noted, although *p*-values are not statistically significant. Third, among oxidative-stress-related genes, mitogen-activated protein kinase 2, which responds primarily to stress and inflammatory stimuli, is significantly upregulated, and the known typical ROS absorber genes, such as those encoding GST-1 and UDP glucuronosyltransferase show mild but significant increases. C3h-dioxin-inducible cytosolic aldehyde dehydrogenase-3, Cytochrome c oxidase Vb, and lactate dehydrogenase are also upregulated. Fourth, among growth-factor-related genes, those encoding the hepatocyte-growth factor-like protein shows significant upregulation, associated with a slight increase/decrease in expression level, with less significant *p*-values, for the following genes: fibroblast growth factor (FGF)-15, FGF-b, G protein-coupled receptor, growth factor-induced delayed-early-response protein, insulin-like growth factor 1 receptor precursor, insulin-induced growth response protein cl-6, tumor growth factor (TGF)-beta 1, TGF-beta 1 masking protein, and tumor necrosis factor alpha. Fifth, among the gene expression profiling of oncogenes, RhoB, which is possibly related to the genotoxic effect of benzene metabolites, shows a high expression level. Finally, hemopoiesis-related genes also show particular changes in their expression level, but the profiling of such genes led to the elucidation that benzene generally induces suppression of cell proliferation without an increase in cytokine gene expression levels.

TABLE 3.—*p53*-related genes whose expression level decreased or increased by benzene exposure, but unchanged in the wild-type mice.

WT: unchanged *p53*-KO: decreased	CalDAG-GEFI, Cbfa2, Dctn1, Frl, Grl-1, Ig/EBP, Klra3, Mek5, MEP, Mlp1, B-myb, Nog, PBX2, Prkm3, PTPalpha, Rad50, Rad51, Zfp94
WT: unchanged *p53*-KO: increased	24p3, 4E-BP2, Abcg2, ACRP, Activine, Ahd3, Alp, Anx3, AOE372, Apaf1, BAG-1, BAP, bcl-2, Calcyclin, Canexin, Caspase 9, Caspase 9S, CCR1, CD3 theta, CD71, CD143, Cox5b, Cox7a1, COX8H, Ctla-2a, Cu/Zn-SOD, Cyclin B1, DCIR, Dnmt2, Dpagt2, E4BP4, EPO, FACS, Fes, elk1, G6PD, G6PD-2, Galbp, Gapdh, Gcdh, Gdi2, Growth hormone, Gnb-1, Gng3lg, H-2T18, HES-1, IGF-1, IL1bc, IL-4, IL-9, JSR1, LDH-1, LDH-2, mLigI, Lipo 1, Lrf, Ly-3, Ly-40, Jam, JNK2, Kcc1, KSR1, M-CSF, Mac-1 alpha, Mch6, Mgl1, MHR23A, MmCEN3, Mrad17, MRP14, Mtx2, NFATp, NL, Nmo1, OERK, PAFR, Pde8, PERK, PGRP, Pla2g2c, PLGF, Pop2, Prkm9, Prtn3, RBP-L, Rga, S100A13, Siva, Smad 6, SPRR2J, Stat4, Stat 5B, TCF4, TOM1, Trypsin 2, Tst

See reference, Yoon et al. (2003).

It is of interest to determine gene expression in *p53*-KO mice with or without exposure by benzene inhalation (Yoon et al., 2003). In Table 3, the annotated genes were all downregulated (top) or upregulated (bottom) after benzene exposure, although their expressions were not altered in the wild-type mice, implying that the expressions of these genes are masked by the homeostasis governed by *p53* gene regulation. Thus, this study on *p53*-KO mice led to the elucidation of hidden gene alterations in wild-type mice, which we do not generally observe in toxicological examination.

REFERENCES

Boley, S. E., Wong, V. A., French, J. E., and Recio, L. (2002). *p53* heterozygosity alters the mRNA expression of *p53* target genes in the bone marrow in response to inhaled benzene. *Toxicol Sci* 66, 209–15.

Cronkite, E. P., Bullis, J., Inoue, T., and Drew, R. T. (1984). Benzene inhalation produces leukemia in mice. *Toxicol Appl Pharmacol* 75, 358–61.

Cronkite, E. P., Drew, R. T., Inoue, T., Hirabayashi, Y., and Bullis, E. (1989). Hematotoxicity and carcinogenicity of inhaled benzene. *Environ Health Perspect* 82, 97–108.

Cronkite, E. P., Inoue, T., Carsten, A. L., Miller, M. E., Bullis, J. E., and Drew, R. T. (1982). Effects of benzene inhalation on murine pluripotent stem cells. *J Toxicol Environ Health* 9, 411–21.

Farris, G. M., Robinson, S. N., Gaido, K. W., Wong, B. A., Wong, V. A., Hahn, W. P., and Shah, R. S. (1997). Benzene-induced hematotoxicity and bone marrow compensation in B6C3F1 mice. *Fundam Appl Toxicol* 36, 119–29.

French, J. E., Lacks, G. D., Trempus, C., Dunnick, J. K., Foley, J., Mahler, J., Tice, R. R., and Tennant, R. W. (2001). Loss of heterozygosity frequency at the *Trp53* locus in *p53*-deficient (+/−) mouse tumors is carcinogen- and tissue-dependent. *Carcinogenesis* 22, 99–106.

Hirabayashi, Y., Matsumura, T., Matsuda, M., Kuramoto, K., Motoyoshi, K., Yoshida, K., Sasaki, H., and Inoue, T. (1998). Cell kinetics of hemopoietic colony-forming units in spleen (CFU-S) in young and old mice. *Mech Ageing Dev* 101, 221–31.

Hirabayashi, Y., Yoon, B. I., Kawasaki, Y., Li, G. X., Kanno, J., and Inoue, T. (2002). On the mechanistic differences of benzene-induced leukemogenesis between wild type and *p53* knockout mice. *Molecular Mechanisms for Radiation-Induced Cellular Response and Cancer Development* (K. Tanaka, T. Takabatake, K. Fujikawa, T. Matsumoto, and F. Sado, eds.), pp. 110–16. Aomori, Institute for Environmental Sciences, Japan.

Ho, T. Y., and Witz, G. (1997). Increased gene expression in human promyeloid leukemia cells exposed to trans, trans-muconaldehyde, a hematotoxic benzene metabolite. *Carcinogenesis* 18, 739–44.

Irons, R. D., Heck, H., Moore, B. J., and Muirhead, K. A. (1979). Effects of short-term benzene administration on bone marrow cell cycle kinetics in the rat. *Toxicol Appl Pharmacol* 51, 399–409.

Kawasaki, Y., Hirabayashi, Y., Yoon, B. I., Huo, Y., Kaneko, T., Kurokawa, Y., and Inoue, T. (2001). Benzene inhalation induced an early onset and a high incidence of leukemias in the *p53* deficient C57BL/6 mice. *Jpn J Cancer Res* 92(Suppl), 71.

Lee, E. W., Garner, C. D., and Johnson, J. T. (1988). A proposed role played by benzene itself in the induction of acute cytopenia: inhibition of DNA synthesis. *Res Commun Chem Pathol Pharmacol* 60, 27–46.

Le Noir and Claude (1897). Sur un cas de purpura atribué a l'intoxication par la benzine. *Bull Med Soc Hop Paris* 14, 1251–60.

Li, G. X., Hirabayashi, Y., Yoon, B. I., Kawasaki, Y., Kurokawa, Y., Yodoi, J., Kanno, J., and Inoue, T. (2003). Benzene-induced leukemia is prevented by over-expression of Trx/ADF, along with increase in Trx/ADF-expression, increase in SOD-activity, and decrease in micronuclei. *Cancer Science* 94(suppl), 265.

Mimura, J., Yamashita, K., Nakamura, K., Morita, M., Takagi, T. N., Nakao, K., Ema, M., Sogawa, K., Yasuda, M., Katsuki, M., and Fujii-Kuriyama, Y. (1997). Loss of teratogenic response to 2,3,7,8-tetrachlorodibenzo-*p*-dioxin (TCDD) in mice lacking the Ah (dioxin) receptor. *Genes Cells* 2, 645–54.

Moeschlin, S., and Speck, B. (1967). Experimental studies on the mechanism of action of benzene on the bone marrow (radioautographic studies using 3H-thymidine). *Acta Haematol* 38, 104–11.

Schattenberg, D. G., Stillman, W. S., Gruntmeir, J. J., Helm, K. M., Irons, R. D., and Ross, D. (1994). Peroxidase activity in murine and human hematopoietic progenitor cells: potential relevance to benzene-induced toxicity. *Mol Pharmacol* 46, 346–51.

Snyder, C. A., Goldstein, B. D., Sellakumar, A. R., Bromberg, I., Laskin, S., and Albert, R. E. (1980). The inhalation toxicology of benzene: incidence of hematopoietic neoplasms and hematotoxicity in ARK/J and C57BL/6J mice. *Toxicol Appl Pharmacol* 54, 323–31.

Tsukada, T., Tomooka, Y., Takai, S., Ueda, Y., Nishikawa, S., Yagi, T., Tokunaga, T., Takeda, N., Suda, Y., Abe, S., Matsuo, I., Ikawa, Y., and Aizawa, S. (1993). Enhanced proliferative potential in culture of cells from *p53*-deficient mice. *Oncogene* 8, 3313–22.

Yoon, B. I., Hirabayashi, Y., Kawasaki, Y., Kodama, Y., Kaneko, T., Kim, D. Y., and Inoue, T. (2001). Mechanism of action of benzene toxicity: cell cycle suppression in hemopoietic progenitor cells (CFU-GM). *Exp Hematol* 29, 278–85.

Yoon, B. I., Hirabayashi, Y., Kawasaki, Y., Kodama, Y., Kaneko, T., Kanno, J., Kim, D. Y., Fujii-Kuriyama, Y., and Inoue, T. (2002). Aryl hydrocarbon receptor mediates benzene-induced hematotoxicity. *Toxicol Sci* 70, 150–6.

Yoon, B. I., Li, G. X., Kitada, K., Kawasaki, Y., Igarashi, K., Kodama, Y., Inoue, T., Kobayashi, K., Kanno, J., Kim, D. Y., and Hirabayashi, Y. (2003). Mechanisms of benzene-induced hematotoxicity and leukemogenicity: cDNA microarray analyses using mouse bone marrow tissue. *Environ Health Perspect* 111, 1411–20.

Zhang, S., Cawley, G. F., Eyer, C. S., and Backes, W. L. (2002). Altered ethylbenzene-mediated hepatic CYP2E1 expression in growth hormone-deficient dwarf rats. *Toxicol Appl Pharmacol* 179, 74–82.

Available online at www.sciencedirect.com
SCIENCE DIRECT
Journal of Steroid Biochemistry & Molecular Biology 91 (2004) 121–129
The Journal of Steroid Biochemistry & Molecular Biology
www.elsevier.com/locate/jsbmb

Identification of estrogen-responsive genes in the GH3 cell line by cDNA microarray analysis

Nariaki Fujimoto [a,*], Katsuhide Igarashi [b], Junn Kanno [b], Hiroaki Honda [a], Tohru Inoue [b]

[a] *Department of Developmental Biology, Research Institute for Radiation Biology and Medicine (RIRBM), Hiroshima University, 1-2-3 Kasumi, Minami-ku, Hiroshima 734-8553, Japan*

[b] *Biological Safety Research Center, National Institute of Health Sciences, Kamiyoga 1-18-1, Setagaya-ku, Tokyo 158-8501, Japan*

Received 20 October 2003; accepted 27 February 2004

Abstract

To identify estrogen-responsive genes in somatolactotrophic cells of the pituitary gland, a rat pituitary cell line GH3 was subjected to cDNA microarray analysis. GH3 cells respond to estrogen by growth as well as prolactin synthesis. RNAs extracted from GH3 cells treated with 17β-estradiol (E2) at 10^{-9} M for 24 h were compared with the control samples. The effect of an antiestrogen ICI182780 was also examined. The array analysis indicated 26 genes to be up-regulated and only seven genes down-regulated by E2. Fourteen genes were further examined by real-time RT-PCR quantification and 10 were confirmed to be regulated by the hormone in a dose-dependent manner. Expression and regulation of these genes were then examined in the anterior pituitary glands of female F344 rats ovariectomized and/or treated with E2 and 8 out of 10 were again found to be up-regulated. Interestingly, two of the most estrogen-responsive genes in GH3 cells were strongly dependent on E2 in vivo. #1 was identified as calbindin-D9k mRNA, with 80- and 118-fold induction over the ovariectomized controls at 3 and 24 h, respectively, after E2 administration. #2 was found to be parvalbumin mRNA, with 30-fold increase at 24 h. Third was c-*myc* mRNA, with 4.5 times induction at 24 h. The levels were maintained after one month of chronic E2 treatment. Identification of these estrogen-responsive genes should contribute to understating of estrogen actions in the pituitary gland.

Keywords: Estrogen-responsive genes; cDNA microarray; Pituitary; GH3; Rats

1. Introduction

Estrogen regulates multiple functions in different cell types in the anterior pituitary gland [1–3]. In the somatolactotrophs (GH/prolactin cells), it is well documented that estrogen activates prolactin mRNA transcription through the estrogen-responsive element (ERE) located in the 5′-upstream regulatory region [4,5]. The storage and release of prolactin are also regulated by estrogen [6]. In addition to hormone production, estrogen promotes cell proliferation in somatolactotrophs, which is prominent in the rat case [7–9]. Although estrogen-responsive expression of a series of genes must be involved in these biological functions of the pituitary cells, only a few have so far been reported to be regulated by estrogen [2].

GH3 is a widely used rat pituitary somatolactotrophic cell line, originally isolated from the MtT/W5 pituitary tumor, whose growth and prolactin synthesis are stimulated by estrogen [10,11]. There is a variation in the estrogen-responsiveness of this cell line reported in the literature [5,12–15], but the cells obtained from the Health Science Research Resources Bank in Osaka, Japan, display high sensitivity with regard to induction of cell proliferation. In the present study, we performed a gene expression analysis of estrogen action in GH3 cells using the cDNA microarray technique and found many of the identified estrogen-responsive genes to also be similarly regulated in vivo in the anterior pituitary in F344 rats.

2. Materials and methods

2.1. Chemicals

17β-estradiol (E2) was purchased from Sigma Chemicals, St. Louis, MO, USA and ICI182780 was obtained from Tocris Cookson Ltd., Bristol, UK. Each was dissolved in

* Corresponding author. Tel.: +81 82 257 5820; fax: +81 82 256 7107.
E-mail address: nfjm@hiroshima-u.ac.jp (N. Fujimoto).

0960-0760/$ – see front matter © 2004 Elsevier Ltd. All rights reserved.
doi:10.1016/j.jsbmb.2004.02.006